ELSEVIER

Journal of Physics and Chemistry of Solids 65 (2004) 995–1003

JOURNAL OF PHYSICS AND CHEMISTRY OF SOLIDS

www.elsevier.com/locate/jpcs

Concerning the cation distribution in $MnFe_2O_4$ synthesized through the thermal decomposition of oxalates

M.A. Gabal[a,*], S.S. Ata-Allah[b]

[a]*Department of Chemistry, Faculty of Science, Benha University, Benha, Egypt*
[b]*Reactor and Neutron Physics Department, Nuclear Research Center, Atomic Energy Authority, Cairo, Egypt*

Received 12 June 2003; revised 7 October 2003; accepted 15 October 2003

Abstract

A single phase manganese ferrite powder have been synthesized through the thermal decomposition reaction of $MnC_2O_4{\cdot}2H_2O$–$FeC_2O_4{\cdot}2H_2O$ (1:2 mole ratio) mixture in air. DTA-TG, XRD, Mössbauer spectroscopy, FT-IR and SEM techniques were used to investigate the effect of calcination temperature on the mixture. Firing of the mixture in the range 300–500 °C produce ultra-fine particles of α-Fe_2O_3 having paramagnetic properties. XRD, Mössbauer spectroscopy as well as SEM experiments showed the progressive increase in the particle size of α-Fe_2O_3 up to 500 °C. DTA study reveals an exothermic phase transition at 550 °C attributed to the formation of a Fe_2O_3–Mn_2O_3 solid solution which persists to appear up to 1000 °C. At 1100 °C, the single phase $MnFe_2O_4$ with a cubic structure predominated. The Mössbauer effect spectrum of the produced ferrite exhibits normal Zeeman split sextets due to Fe^{3+}ions at tetrahedral (A) and octahedral (B) sites. The obtained cation distribution from Mössbauer spectroscopy is $(Fe_{0.92}Mn_{0.08})[Fe_{1.08}Mn_{0.92}]O_4$.

Keywords: C. Mössbauer spectroscopy

1. Introduction

Transition metal ferrites are a family of oxides having great technological importance because of their novel physical properties. They can be used in the fabrication of magnetic, electronic and microwave devices such as thermistors and recording media [1]. The basis for the wide range of applications is related to the variety of transition metal cations that can be incorporated into the lattice of the parent magnetite structure. The majority of the spinel ferrites belong to the space group *Fd*3*m* with lattice parameters around 8.5 Å [2].

The cation distribution of these materials has the form: $(Fe_{\delta}^{3+}M_{1-\delta}^{2+})[M_{\delta}^{2+}Fe_{2-\delta}^{3+}]O_4^{2-}$ where the round and the square brackets represent the tetrahedral (A) and the octahedral (B) sites, respectively. Occupation of the tetrahedral site entirely with a divalent transition metal (i.e. $\delta = 0$) yields a normal spinel structure, while occupation of the octahedral site with the divalent transition metal (i.e. $\delta = 1$) produces an inverse spinel structure. The determination of the cation distribution in the tetrahedral and octahedral sites can be achieved using neutron diffraction or Mössbauer spectroscopy techniques, and has been the subject of many studies [3,4].

In technologies where ferrites are to be used for magnetic or electrical applications, high-density materials are generally required. So, ferrites are often prepared by high-temperature solid-state reactions between finely ground powders [5]. Alternatively, several coprecipitated precursor systems have been used, including oxalates [6], formates [7] and hydrazinates [8]. The freeze-drying method [9] can be used also to make various forms such as poly crystalline, aggregates, thin and thick films and single crystals.

Manganese ferrite ($MnFe_2O_4$) was originally thought to be an inverse spinel but was later found to be about 80% normal, 20% inverse. However, since both cations ($Mn^{2+}$and Fe^{3+}) are d^5 transition elements, the overall magnetic moment is insensitive to the degree of inversion. It is a well-known soft magnetic material due to its low coercivety and moderate saturation magnetization as well as a remarkable chemical stability and a mechanical hardness [10].

Extensive studies on the preparation and characterization of manganese ferrite have been reported giving useful information about the influence of the preparation method

* Corresponding author. Present address: Institute of Mechanical Engineering and Mechanics (IMVM), University of Karlsruhe, Geb. 30.70, Kaiser Str. 12, Karlsruhe 76128, Germany. Tel.: +20-1010-48600; fax: +20-132-22578.

E-mail address: mgabalabdo@yahoo.com (M.A. Gabal).

0022-3697/$ - see front matter © 2003 Elsevier Ltd. All rights reserved.
doi:10.1016/j.jpcs.2003.10.059

on the various physical properties. The solid-solid interaction between manganese carbonate and ferric oxide have been investigated by Deraz and El-Shobaky [11] using DTA and X-ray powder diffraction (XRD) techniques. It was found that $MnFe_2O_4$ starts to appear at temperatures starting from 900 °C. The nanocrystalline $MnFe_2O_4$ phase [12], prepared by the ball milling of Mn_2O_3 and Fe_2O_3 under an argon atmosphere, was formed after annealing at 600–700 °C. Using the hydrothermal route at pH 9 and 210 °C, a nanosized manganese ferrite was prepared and studied using XRD, magnetization measurements and Mössbauer spectroscopy [13]. Burojeanu et al. [14] have been prepared $MnFe_2O_4$ by coprecipitation from a MnO_2 and $FeSO_4{\cdot}7H_2O$ aqueous solution, and the produced ferrite was characterized using DTA-TG, DTG, IR, mass spectral, SEM and XRD measurements.

The present study has focused on the use of an oxalates system for the preparation of manganese ferrite with high-purity through the thermal decomposition reaction taking place between the solid-state oxalates mixture of $MnC_2O_4{\cdot}2H_2O$–$FeC_2O_4{\cdot}2H_2O$ (1:2 mole ratio) in air. DTA-TG, XRD, Mössbauer spectroscopy, FT-IR and SEM techniques were used to characterize the decomposition products obtained at different temperatures as well as the ferrite formation. DTA-TG measurements provide information about the thermal decomposition course of the mixture, and indicate the temperatures required for the calcinations processes. XRD, Mössbauer, FT-IR and SEM measurements were used to identify phases formation and the changing in the particle sizes along the decomposition course. Mössbauer spectroscopy was also used to study the cation distribution and hyperfine fields at both (A) and (B) sites in the formed $MnFe_2O_4$ spinel.

2. Experimental

2.1. Materials

Individual metal oxalates of $MnC_2O_4{\cdot}2H_2O$ and $FeC_2O_4{\cdot}2H_2O$ were prepared by the coprecipitation technique. Weighed amounts of high purity $MnCl_2{\cdot}4H_2O$ or $FeSO_4{\cdot}7H_2O$ was dissolved in deionized water, and then oxalic acid solution (which contains an equivalent amount) was added slowly with vigorous stirring untill a permanent precipitate occurred. The precipitate was filtered, washed with distilled water, and allowed to dry in air.

Mixed metal oxalates ($MnC_2O_4{\cdot}2H_2O$–$FeC_2O_4{\cdot}2H_2O$ with a 1:2 mole ratio) was prepared by the impregnation technique described previously [15].

To characterize the products at different decomposition stages and to follow the ferrite formation, samples of the mixture were calcined at different temperatures (estimated from DTA-TG results) for different time durations in a Pt crucibles under static air atmosphere. Thus samples of the mixture were thermally heated in a muffle furnace for 5 min at temperatures ranging from 300 to 1000 °C with an interval of 100 °C or for 2 h at 1100 °C. Samples were then removed from the furnace, and cooled down to room temperature in a desiccator.

For the sake of simplicity, these products are denoted in the text by the notation MnFe followed by the calcination temperature. Thus, MnFe-300 indicates the decomposition product of MnFe at 300 °C.

2.2. Techniques

Thermal analysis experiments including differential thermal analysis (DTA) and thermogravimetry (TG) were carried out using a Shimadzu DT-40 thermal analyzer (Japan). The experiment was performed in a dynamic (30 ml min^{-1}) atmosphere of air up to 1100 °C at a heating rate of 5 °C min^{-1} using a sample mass of 10 mg. Highly sintered α-Al_2O_3 powder was used as the reference material for the DTA measurements.

XRD was carried out using a model PW 1710 Philips diffractometer at ambient temperature. The instrument is equipped with an iron anode generating Fe Kα_1 radiation ($\lambda = 1.9374$ Å). For identification purposes, the relative intensities (I/I_0) and the d-spacing (Å) were compared with standard diffraction patterns in the ASTM powder diffraction files [16].

Fourier transform-infrared spectra (FT-IR) were measured between 4000 and 200 cm^{-1} using a KBr disc technique with a model FT-IR 310 Jasco spectrometer (Japan). In all spectra, the relative transmittance was represented versus wavenumber (cm^{-1}).

The Mössbauer spectra at room temperature were recorded on an Austin Science Mössbauer effect spectrometer using a constant acceleration derive and a 1024-channel analyzer. The source was ^{57}Co in Rh matrix with an intial activity of 50 mCi. The absorber contained 10 mg of Fe cm^{-2}. The Mössbauer parameters were computed using an interactive least square 'Mos-90' program [17].

SEM measurements were performed using a Jeol T 300 (Japan) scanning electron microscope operated at 15 keV. Mixtures were mounted separately on aluminum substrates evacuated to 10^3 Torr, and were precoated (20, 5 min for each side of the four sides) in a sputter-coater with a thin uniform gold/palladium film to minimize charging in the electron beam. The applied voltage was 1.2–1.6 kV.

3. Results and discussion

3.1. Thermal decomposition course

Typical DTA-TG curves for a $MnC_2O_4{\cdot}2H_2O$–$FeC_2O_4{\cdot}2H_2O$ (1:2 mole ratio) mixture at heating rate of 5 °C min^{-1} in air atmosphere is shown in Fig. 1. The TG curve indicates multistep weight loss when increasing

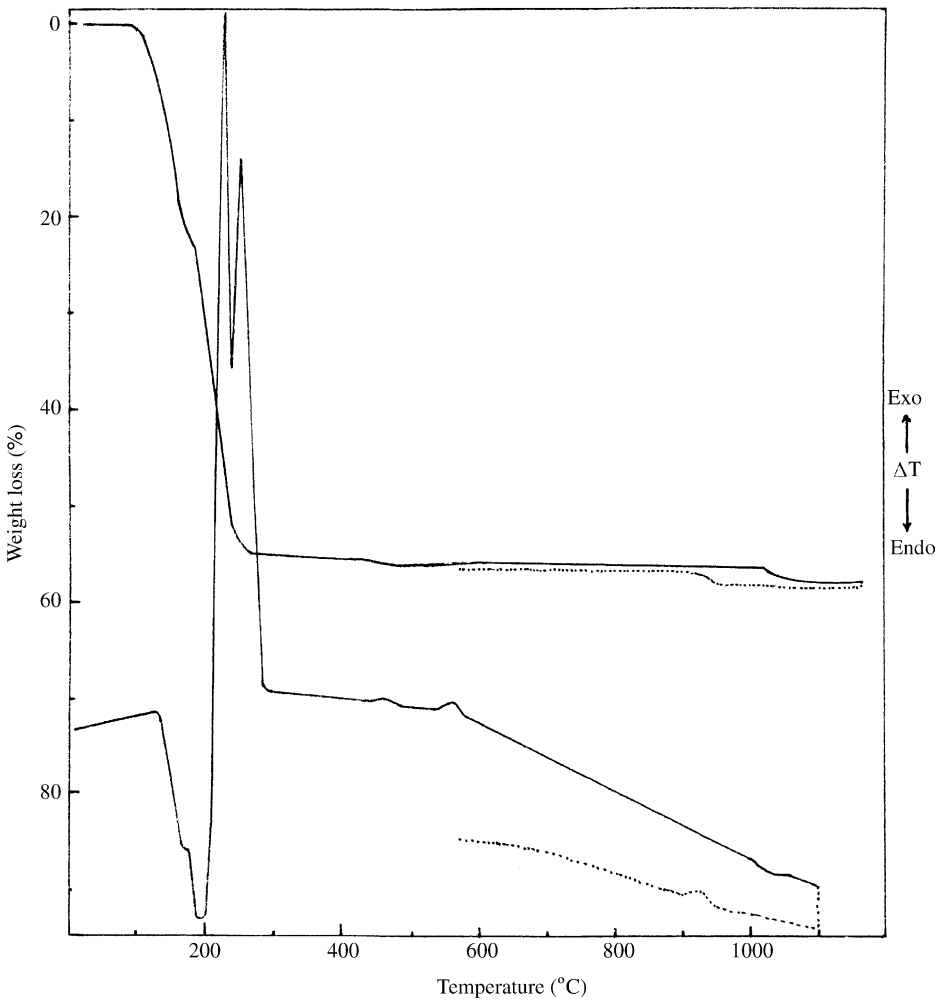

Fig. 1. DTA–TG curves of $MnC_2O_4{\cdot}2H_2O$–$FeC_2O_4{\cdot}2H_2O$ (1:2 mole ratio) mixture in air at a specified heating rate of 5 °C min^{-1}.

the temperature up to 1100 °C. Considerable weight loss (about 54.5%) occurred in the temperature range 117–260 °C through two overlapped steps. The first one is accompanied by a large dehydration endothermic DTA peak at 193 °C with a slight shoulder on its low-temperature side (at 170 °C). The weight loss effected in this step (about 20%) accounts for the complete dehydration of the mixture and the formation of anhydrous oxalate mixture (expected weight loss = 20%).

The endothermic dehydration peak was swamped by two large exothermic peaks (at 210 and 260 °C) closely corresponding to the second step (observed weight loss 34.5%) which follows immediately after the completion of the first one. This indicates that the decomposition of the anhydrous mixture occurs virtually in two unresolved stages. On the basis of the DTA peak's values, the first one is attributed to the oxidative decomposition of FeC_2O_4 to Fe_2O_3 and the second one is attributed to the oxidative decomposition of MnC_2O_4 [18]. Using X-ray diffraction, Macklen [18] proposed that the decomposition product of manganese oxalate at this temperature range possesses a poorly defined structure and identification is not possible. If however, the temperature is raised further, the sample undergoes a further small exothermic weight loss between 437 and 470 °C to yield a product that can be identified by XRD as Mn_2O_3. Consistent with this result, a very small exothermic weight loss (1.5%) was obtained by raising the temperature up to about 450 °C. The weight loss after this decomposition step was brought to 56%, which is close to that expected (55.6%) for the overall conversion of the mixture to a Fe_2O_3–Mn_2O_3 mixture.

The exothermic DTA peak which appears at 550 °C can be attributed to the formation of iron-manganese oxide solid solution [$(Fe,Mn)_2O_3$]. This solid solution is thermally stable up to the last decomposition step in which the Mn_2O_3 dissociated to Mn_3O_4. This step is accompanied by a weight loss of 1.5% (theoretical weight loss is 1.5%) at 1050 °C. A small endothermic DTA peak at 1020 °C characterized this step. Macklen [18] showed that the conversion of Mn_2O_3 to Mn_3O_4 occurs between 910 and 950 °C. The higher conversion temperature obtained in this work is attributed to the presence of Mn_2O_3 in a solid solution with Fe_2O_3. The heating process was continued up to 1100 °C, and then the mixture was cooled in air up to 800 °C. The cooling DTA-TG

curves were represented by the dotted lines (see Fig. 1). A reverse behavior for that obtained on heating was obtained where the TG curve shows a weight gain accompanied by a small exothermic DTA peak at 920 °C. This behavior is attributed to the conversion of Mn_3O_4 to Mn_2O_3, and indicates the inability of obtaining $MnFe_2O_4$ spinel without isothermal calcination at temperature higher than 1050 °C.

3.2. X-ray powder diffraction

XRD patterns taken at room temperature of MnFx mixture and its calcined products at different temperatures are illustrated in Fig. 2. In this figure, the effect of the calcination temperature on the composition and crystallinity was significant. XRD of the parent mixture shows broad peaks characteristic for the individual oxalates of $MnC_2O_4{\cdot}2H_2O$ (JCPDS file no. 25-544) and $FeC_2O_4{\cdot}2H_2O$ (JCPDS file no. 23-293). These characteristic peaks disappeared by raising the calcination temperature to 300 °C. A nearly amorphous XRD pattern was obtained for MnFx-300 mixture (see Fig. 2b) which suggested that the mixture at this decomposition stage possesses a very weak crystallinity. A few diffused and broad peaks were observed by raising the calcination temperature to 400 °C (see Fig. 2c). However, the considerable broadening of all of the diffraction peaks suggests that the particle size of

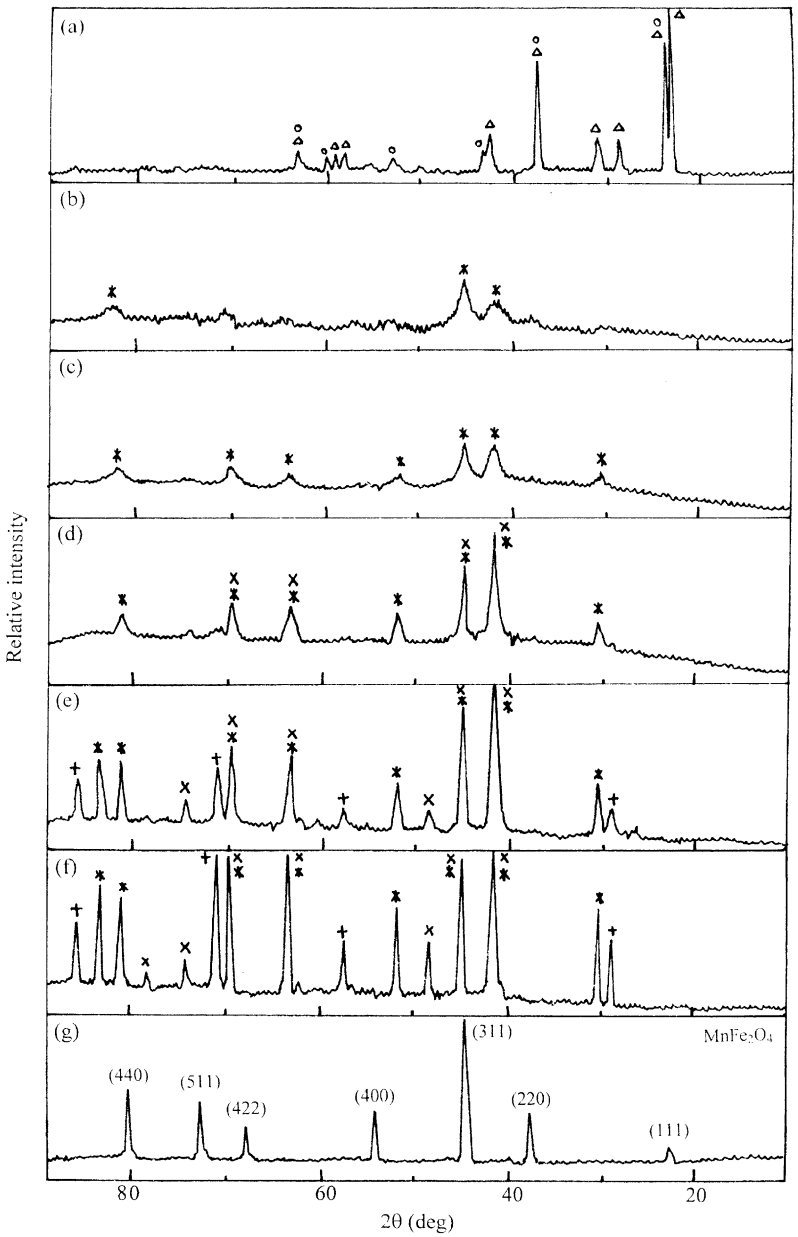

Fig. 2. Characteristic parts of XRD patterns of $MnC_2O_4{\cdot}2H_2O$–$FeC_2O_4{\cdot}2H_2O$ (1:2 mole ratio) mixture calcined at different temperatures. (a) Parent mixture, (b) mixture calcined at 300 °C, (c) mixture calcined at 400 °C, (d) mixture calcined at 500 °C, (e) mixture calcined at 600 °C, (f) mixture calcined at 1000 °C and (g) mixture calcined at 1100 °C. Phases: (△) $MnC_2O_4{\cdot}2H_2O$, (○) $FeC_2O_4{\cdot}2H_2O$, (∗) α-Fe_2O_3, (×) γ-Mn_2O_3, (+) $(Fe,Mn)_2O_3$.

the mixture is expected to remain very small. It is evident that the increase in the annealing temperature will yield a decrease in the broadening of the major peaks with an increase in their intensities which reflects an evolution in the crystallinity. Consistent with these the MnFe-500 mixture gave an XRD pattern (see Fig. 2d) with improved crystallinity, showing characteristic peaks of α-Fe_2O_3 (JCPDS file no. 13-534) and γ-Mn_2O_3 (JCPDS file no. 18-803). The sharpness and intensity of the characteristic peaks of α-Fe_2O_3 and γ-Mn_2O_3 increase with increasing calcination temperature beyond 500 °C due to improved crystallinity and particle sizes.

XRD of the 600 °C heated mixture (see Fig. 2e) shows new sharp and diffused peaks at 3.87, 2.01, 1.66 and 1.42 Å which are attributed to a phase transformation occurs in the mixture (in agreement with the exothermic DTA peak at 550 °C). This phase transition is attributed to the formation of iron-manganese oxide solid solution; $(Fe,Mn)_2O_3$ [19]. The only change which can be observed by raising the annealing temperature up to 1000 °C is the increase in the intensities of the characteristic peaks of the $(Fe,Mn)_2O_3$ solid solution. This is obvious from the XRD pattern of the MnFe-1000 mixture (see Fig. 2f).

The XRD pattern of theMnFe-1100 mixture (see Fig. 2g) indicates the formation of a single phase spinel with the cubic structure of $MnFe_2O_4$ (jacobsite) (JCPDS file no. 10-319). The calculated lattice parameter ($a = 8.45$ Å) agree well with that reported [20].

3.3. Mössbauer spectral studies

^{57}Fe Mössbauer absorption spectra measured at room temperature for the non-calcined MnFe mixture and mixtures calcined at different temperatures are shown in Fig. 3. The black dots represent experimental points and the continuous lines through the data points are results of the least square fit to the data. The Mössbauer parameters obtained such as the isomer shift (δ), the quadrupole splitting (ΔE_Q), the spectral line width (Γ) and the hyperfine fields (H) are reported in Table 1.

The Mössbauer spectrum of the parent mixture; MnFe (see Fig. 3a) do not reveal any magnetic interaction, and shows a doublet with a large positive isomer shift and quadrupole splitting as indication of divalent iron. Brady and Duncan [21] reported an isomer shift and quadrupole splitting of 1.02 and 1.7 mm s^{-1}, respectively, for $FeC_2O_4{\cdot}2H_2O$ at room temperature which are in excellent agreement with the values obtained in this paper (see Table 1).

The spectra of all of the samples annealed at temperatures ranging from 300 to 1000 °C (see Fig. 3b–f) consist of a six-line subspectra and an absorption of a central quadrupole doublet having a very small magnetically split pattern. The thermal analysis data inferred that the early stages of the decomposition involved the oxidation of iron(II) to iron(III). This is clearly proven by the spectrum

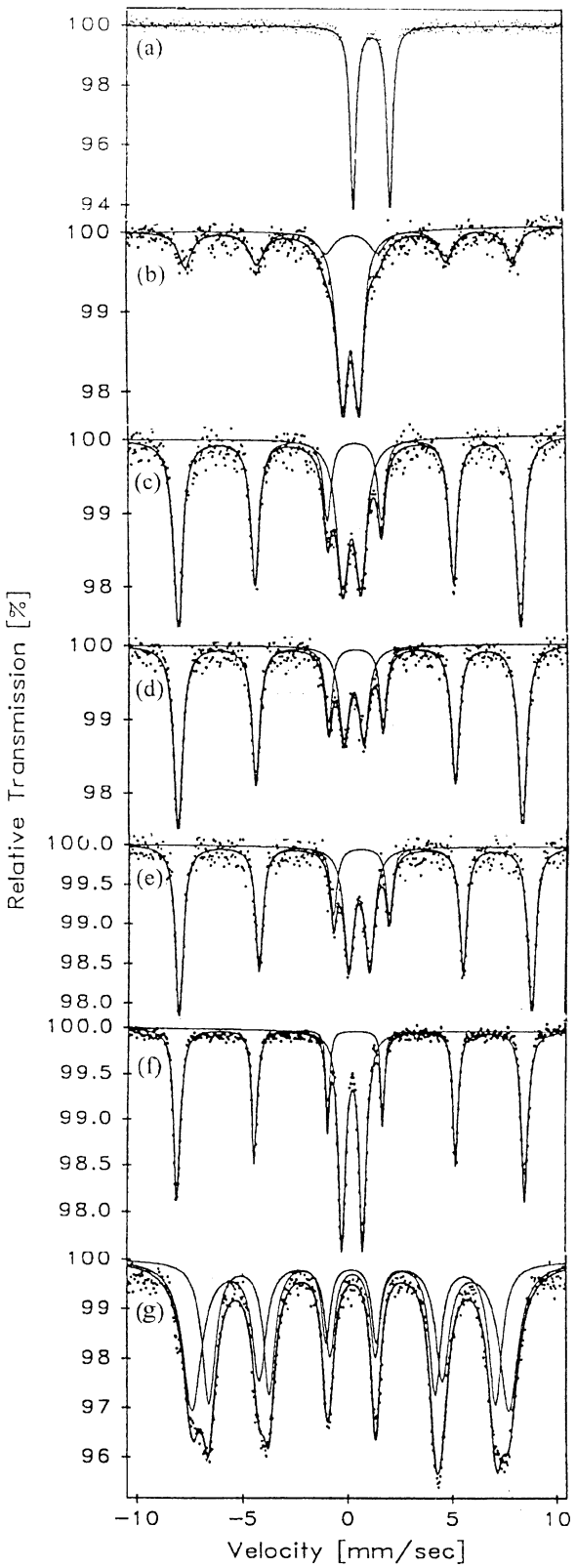

Fig. 3. The Mössbauer spectra of $MnC_2O_4{\cdot}2H_2O$–$FeC_2O_4{\cdot}2H_2O$ (1:2 mole ratio) mixture calcined at different temperatures: (a) Parent mixture, (b) mixture calcined at 300 °C, (c) mixture calcined at 500 °C, (d) mixture calcined at 600 °C, (e) mixture calcined at 800 °C, (f) mixture calcined at 1000 °C and (g) mixture calcined at 1100 °C.

Table 1
Mössbauer parameters for $MnC_2O_4{\cdot}2H_2O$–$FeC_2O_4{\cdot}2H_2O$ (1:2 mole ratio) mixture calcined at different temperatures

Mixture	Subspectra	Area	Isomer shift, δ (± 0.02 mm s^{-1})	Quadrupole splitting, ΔE_Q (± 0.02 mm s^{-1})	Line width, Γ (mm s^{-1})	Hyperfine field, H (± 2 kOe)
MnFe	Doublet	100	1.01	1.70	0.62	–
MnFe-300	Doublet	57	0.42	0.87	0.63	–
	Sextet	43	0.47	0.13	0.75	486
MnFe-400	Doublet	36	0.42	0.88	0.66	–
	Sextet	64	0.44	0.20	0.58	502
MnFe-500	Doublet	31	0.42	0.87	0.68	–
	Sextet	69	0.44	0.23	0.50	508
MnFe-600	Doublet	22	0.46	0.95	0.58	–
	Sextet	78	0.44	0.23	0.48	510
MnFe-700	Doublet	27	0.47	0.95	0.53	–
	Sextet	73	0.44	0.23	0.45	510
MnFe-800	Doublet	30	0.46	0.97	0.54	–
	Sextet	70	0.45	0.23	0.42	510
MnFe-900	Doublet	33	0.46	0.98	0.56	–
	Sextet	67	0.45	0.23	0.42	510
MnFe-1000	Doublet	41	0.46	0.99	0.40	–
	Sextet	59	0.52	0.17	0.37	516
MnFe-1100	(A) site	46	0.41	0.01	0.76	424
	(B) site	54	0.48	0.01	1.08	469

shown in Fig. 3b. The figure shows that the iron(III) oxide formed at 300 °C is of a paramagnetic and ferromagnetic nature, simultaneously. Since it is well known that the magnetic properties are related to the variation of the particle size, then part of Fe_2O_3 possesses an ultrafine particles which give rise to the superparamagnetic relaxation that causes the collapse of the sextet pattern with the formation of a doublet. The other part has an enough large size to maintain the ferromagnetic properties that yields the sextet pattern. A similar results were obtained for CoC_2O_4–FeC_2O_4 [15] and NiC_2O_4–FeC_2O_4 [22] mixtures calcined at 280 and 350 °C, respectively. Since the ratio of the different magnetic phases is based on the calculated absorption ratio of the two subspectra, thus by calculating the area under the doublet subspectra, it was found that (see Table 1) the ratio of the doublet decreases with increasing the annealing temperature up to 500 °C. This is mainly attributed to the effect of the annealing temperature on the crystallinity of α-Fe_2O_3 in agreement with the previous results obtained using XRD analysis. The observed hyperfine magnetic splitting of all of the mixtures up to 500 °C is significantly less than the normal value of iron(III) oxide of 515 kOe [22].

The mixture heated at 600 °C (see Fig. 3d) shows a sextet superimposed on a doublet which possess new Mössbauer parameters other than those obtained for samples calcined at $\leq$500 °C indicating formation of a new phase. The sextet possessing Mössbauer parameters is consistent with those obtained at $\leq$500 °C and attributed again to α-Fe_2O_3. The doublet obtained for this heat-treated mixture is attributed to the reaction between α-Fe_2O_3 and γ-Mn_2O_3 to form a $(Fe,Mn)_2O_3$ solid solution [19]. This doublet persists even upon raising the calcination temperature up to 1000 °C with increasing its ratio, which suggested that more α-Fe_2O_3 reacts with γ-Mn_2O_3 to form $(Fe,Mn)_2O_3$ solid solution upon raising the calcination temperature. Alternatively, the ratio of the sextet subspectra (related to the unreacted α-Fe_2O_3 with γ-Mn_2O_3) decreases upon increasing the calcination temperature. The hyperfine magnetic splitting obtained at 1000 °C (see Table 1) is close to that reported in the literature for α-Fe_2O_3 [22].

The Mössbauer spectrum of the mixture annealed at 1100 °C (see Fig. 3g) shows only a well defined hyperfine Zeemann spectra which can be resolved into two sextets corresponding to tetrahedral and octahedral sites in the $MnFe_2O_4$ spinel. The isomer shift and the line width as well as the hyperfine field are a useful parameters in identifying the subspectra due to tetrahedral and octahedral sites of Fe^{3+}ions. The Zeeman pattern with the smaller isomer shift exhibits the smaller hyperfine fields and for most magnetically ordered spinel ferrites, the magnetic hyperfine field due to Fe^{3+} at A-site is usually smaller than that at B-site. Consequently, the A-site Fe^{3+} isomer shift is found to be more negative than that for the B-site Fe^{3+} ions due to the larger covalency of Fe^{3+} in the A-site. The line width of the tetrahedral component must be less than that of the octahedral component due to the presence of multiple hyperfine fields at the Fe^{3+}nuclei on the octahedral component [23]. On the basis of these points and with reference to Table 1, the sextets with hyperfine fields of 424 and 469 kOe are assigned to Fe^{3+} ions at tetrahedral and octahedral sites, respectively, in agreement with the results obtained by Geller et. al. [24].

The fraction of Fe^{3+}ions at (A) and (B) sites were determined using the areas of Mössbauer subspectra. Thus, considering Table 1, the probable cation distribution of the manganese ferrite is suggested as $(Fe_{0.92}Mn_{0.08})$

$[Fe_{1.08}Mn_{0.92}]O_4$. The difference in the cation distribution of $MnFe_2O_4$ spinel in this work than that reported in Ref. [20] ($(Fe_{0.20}Mn_{0.80})[Fe_{1.80}Mn_{0.20}]O_4$) can be attributed to the method of preparation used in our work which involves a quenching process at 1100 °C.

3.4. FT-IR spectroscopy

The vibrational spectroscopy is considered to be a very useful technique for detection of chemical and structural changes. Fig. 4 displays the FT-IR spectra of the heat-treated MnFe mixture at different temperatures.

Fig. 4a shows the characteristic bands for symmetric and asymmetric O–C–O stretcheing modes at (1317 and 1362 cm^{-1}) and (1632 cm^{-1}), respectively. Also the characteristic bending modes for C=C–O and O–C–O were observed at 812 and 493 cm^{-1}, respectively. The appearance of these above mentioned bands agrees with the presence of the oxalate moiety [25]. The presence of water within the crystal structure of oxalates was revealed by the characteristic bands at 3421 and 1632 cm^{-1}, identified as O–H stretching and bending modes of vibration, respectively.

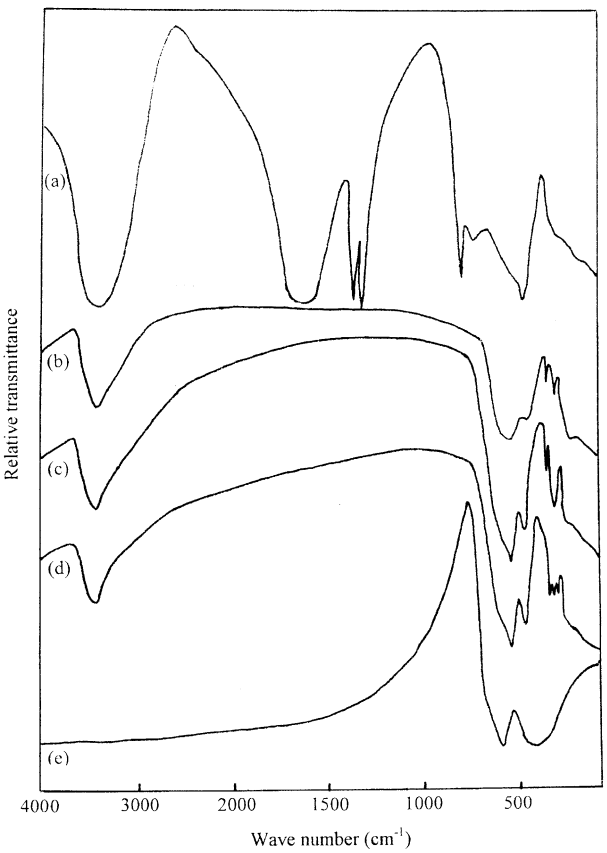

Fig. 4. FT-IR spectra of $MnC_2O_4{\cdot}2H_2O$–$FeC_2O_4{\cdot}2H_2O$ (1:2 mole ratio) mixture calcined at different temperatures: (a) Parent mixture, (b) mixture calcined at 300 °C, (c) mixture calcined at 500 °C, (d) mixture calcined at 600 °C and (e) mixture calcined at 1100 °C.

The disappearance of all of the characteristic bands of the oxalate moiety by raising the calcination temperature up to 300 °C (see Fig. 4b) indicates the complete decomposition of the oxalates. The degree of crystallinity strongly affects the infrared spectra of the hematite. The infrared spectrum of poorly crystalline hematite is characterized by three strong absorption bands at 530, 445 and 308 cm^{-1} which are assigned to O^{2-} displacement [26]. Thus, the broad bands obtained at 540 and 450 cm^{-1} (see Fig. 4b) can be assigned to the presence of poorly crystalline (or possibly amorphous) α-Fe_2O_3. The characteristic O–H bands still appeared at 3421 and 1637 cm^{-1} and are attributed to the adsorption of water molecules by ultra-fine granules of α-Fe_2O_3. These bands persist even upon raising the calcination temperature up to 600 °C.

With progressive increase in the calcination temperature, the resolution and sharpness of the bands increase. This can be ascribed to better crystallinity. The appearance of the bands at 532, 460, 350 and 305 cm^{-1} (see Fig. 4c), on increasing the calcination temperature to 500 °C, indicated that iron(III) oxide crystallinity was improved. Shwertmann and Taylor [27] reported the characteristic infrared bands for well crystallized α-Fe_2O_3 at 540, 470, 345 and 308 cm^{-1}. The small shift in the locations of these characteristic bands obtained can be attributed to the presence of foreign ions (manganese ions) in the α-Fe_2O_3 structure.

The FT-IR spectrum of MnFe-600 mixture (see Fig. 4d) shows that the band at 305 cm^{-1} was replaced by three small bands in the temperature range 300–350 cm^{-1}. This behavior can be attributed to the formation of a new phase besides the α-Fe_2O_3 phase.

The bands appeared at 556 and 380 cm^{-1} for MnFe-1100 mixture are assigned to the stretching vibrations of Fe^{3+}–O^{2-} in the tetrahedral and octahedral complexes of $MnFe_2O_4$, respectively [20].

3.5. Scanning electron microscopy

In this section, SEM micrographs illustrating the change in morphology and texture taking place during the thermal decomposition of MnFe mixture are shown in Fig. 5. It is evident from the micrographs that the particle sizes and shape change throughout the decomposition course. Textural feature resolution of the parent mixture is unsatisfactory because of the very small crystallites size (<0.5 μm). For this reason, the SEM micrograph of the parent mixture is not reproduced here.

The decomposition of the mixture at 300 °C (see Fig. 5a) produces a large number of a small and fine granules with superficial roughening of the crystal edges. This result agrees with the amorphous X-ray diffraction pattern obtained for the mixture at this calcination temperature. Consistent with the FT-IR spectral data, some fine granules of iron oxide absorb moisture from the atmosphere and produce a gelatinous appearance.

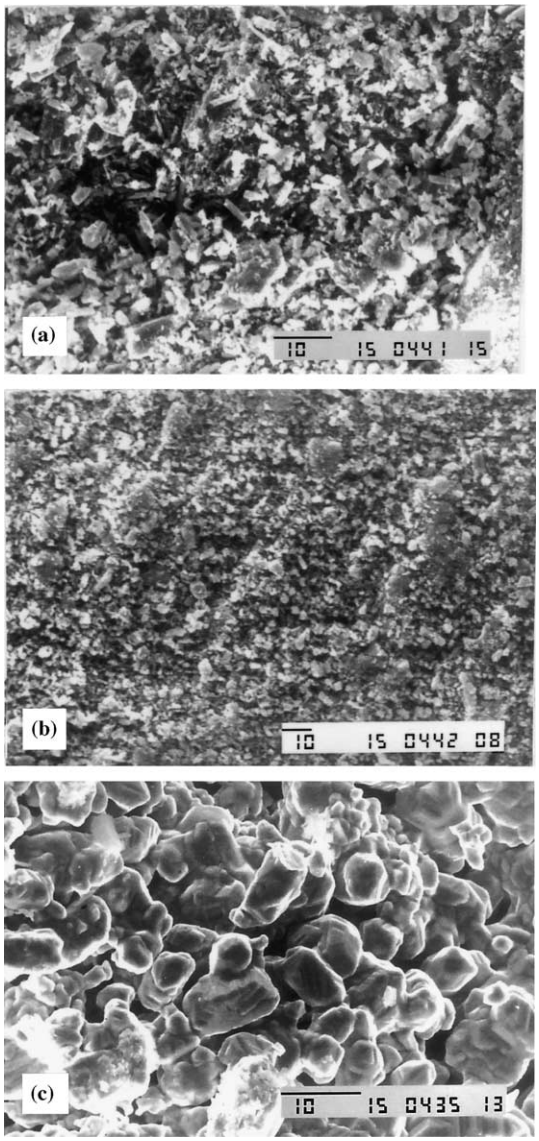

Fig. 5. Scanning electron micrograph showing the changes in texture and morphology that accompany the thermal decomposition of $MnC_2O_4{\cdot}2H_2O$–$FeC_2O_4{\cdot}2H_2O$ (1:2 mole ratio) mixture in air. (a) Mixture calcined at 300 °C, (b) mixture calcined at 500 °C and (c) mixture calcined at 1100 °C (scale bar 10 μm).

Raising the calcination temperature to 500 °C (see Fig. 5b), the fine granules were re-textured into aggregates of crystallites showing some irregularity of shape. Some small granules are present with a gelatinous appearance.

At 1100 °C (see Fig. 5c), the crystallites were coalesced into large aggregates of cubic symmetrical structure characteristic of $MnFe_2O_4$ spinel.

4. Conclusions

The thermal decomposition of the $MnC_2O_4{\cdot}2H_2O$–$FeC_2O_4{\cdot}2H_2O$ (1:2 mole ratio) mixture was found to be an effective method for preparing stoichiometric manganese ferrite of high chemical purity. Changing the temperature for the decomposition of the oxalate mixture has a significant impact on the decomposition and morphology of the decomposition products during the decomposition. Evidence obtained from XRD, FT-IR and Mössbauer data indicates that the ultra-fine particles of α-Fe_2O_3 formed at early stages of the decomposition was of a ferromagnetic and paramagnetic nature, simultaneously, and begin to grow by raising the calcination temperature up to 500 °C as revealed from SEM data. The DTA curve shows an exothermic phase transition at 550 °C attributed to the formation of Fe_2O_3–Mn_2O_3 solid solution which was also detected using XRD and Mössbauer data. At 1100 °C, single phase manganese ferrite (jacobsite) predominates over the solid solution. A different cation distribution ($(Fe_{0.92}Mn_{0.08})[Fe_{1.08}Mn_{0.92}]O_4$) from that present in the literature was detected using Mössbauer spectroscopy and was attributed to the applied method of preparation.

Acknowledgements

The authors would like to thank Dr A.A. El-Bellihi, Chemistry Department, Faculty of Science, King Abdul Aziz University, Jeddah, KSA, for measuring the DTA-TG experiments.

References

[1] Y. Torii, T. Suziki, K. Kato, Y. Uwamino, B.H. Choi, M.J. Lee, J. Mater. Sci. 31 (1996) 2603.
[2] K.E. Sickafus, J.M. Wills, J. Am. Ceram. Soc. 82 (1999) 3297.
[3] M.K. Fayek, F.M. Sayed Ahmed, S.S. Ata-Allah, M.K. Elnimer, M.F. Moustafa, J. Mater. Sci. 27 (1992) 4813.
[4] M.K. Fayek, S.S. Aa-Allah, H.S. Refai, J. Appl. Phys. 85 (1999) 1.
[5] M.I. Rasels, M.P. Cuautle, V.M. Castano, J. Mater. Sci. 331 (1998) 3665.
[6] G.B. Mc Ata-Allah, D.G. Owen, J. Mater. Sci. 33 (1998) 35.
[7] H. Langbein, S. Christen, G. Bonsdorf, Thermochim. Acta 327 (1999) 173.
[8] K. Suresh, K.C. Patil, J. Solid State Chem. 99 (1992) 12.
[9] F.J. Schnettler, D.W. Johnson, Synthesized Microstructure in Ferrite, Tokyo Press, 1971.
[10] A. Goldman, Modern Ferrite Technology, Marcel Dekker, New York, 1993.
[11] N.M. Deraz, G.M. El-Shobaky, Thermochim. Acta 375 (2001) 137.
[12] J. Dung, P.G. Mccormick, R. Street, J. Mag. Mag. Mater. 171 (1997) 309.
[13] C. Upadhyay, H.C. verma, C. Rath, K.K. Sahu, S. Nand, R.P. Das, N.C. Mishra, J. Alloys Compd 326 (2001) 407.
[14] Y.M. Bujoreanu, E. Segal, Solid State Sci. 3 (2001) 407.
[15] M.A. Gabal, A.A. El-Bellihi, S.S. Ata-Allah, J. Mater. Chem. Phys. 81 (2003) 84.
[16] International Center for Diffraction Data, JCPDS, PDF2 Data Base Swarthmore, PA, USA, 1996.
[17] G. Grosse, Mos-90, Version 2.2, second ed., Oskar-Maria-Graf-Ring, Munchen, 1992.
[18] E.D. Macklen, J. Inorg. Nucl. Chem. 30 (1968) 2689.

[19] K. Parida, A. Samal, D. Das, S.N. Chintalpudi, Thermochim. Acta 325 (1999) 69.
[20] Q. Wei, J. Li, Y. Chen, J. Mater. Sci. 36 (2001) 5115.
[21] P.R. Brady, J.F. Duncan, J. Chem. Soc. (1964) 653.
[22] M.A. Gabal, J. Phys. Chem. Solids 64 (2003) 1375.
[23] S.S. Ata-Allah, M.K. Fayek, H.S. Refai, M.F. Moustafa, J. Solid State Chem. 149 (2000) 434.
[24] S.R. Geller, W.J. Grant, A. Cape, G.P. Epionsa, J. Appl. Phys. 38 (1967) 1457.
[25] V. Moye, K.S. Kane, V.N. Kamat Dalal, J. Mater. Sci: Mater. Elect. 1 (1990) 212.
[26] Sh. Yariv, E. Mendelovici, Appl. Spetrosc. 33 (1979) 410.
[27] U. Schwertmann, R.M. Taylor, Minerals in Soil Environments, Soil Science Society of America, Madison, WI, 1977, p. 145.